JOURNAL OF GEOPHYSICAL RESEARCH, VOL. 89, NO. A11, PAGES 9857-9862, NOVEMBER 1, 1984

Perturbations of Subionospheric LF and MF Signals Due to Whistler-Induced Electron Precipitation Bursts

D. L. CARPENTER, U. S. INAN, M. L. TRIMPI, R. A. HELLIWELL, AND J. P. KATSUFRAKIS

Space, Telecommunications and Radioscience Laboratory, Stanford University, California

First evidence of whistler-induced burst precipitation effects on subionospherically propagating signals in the LF and MF ranges have been observed at Palmer ($L \sim 2.4$) and Siple stations ($L \sim 4.3$), Antarctica. The occurrence rate on a 37.2-kHz LF signal originating in California was usually comparable to that on the more disturbed VLF paths. At Palmer, examples at 37.2 kHz were seen on 70% of the nights during a March–April 1983 observing period. Perturbations on a $\sim$ 1800 km-long 780-kHz MF path to Palmer occurred on nights of high activity on VLF paths, but fewer than 10 MF events were usually detected as compared to >50 on the active VLF paths. The MF perturbations were of order 50% in amplitude and were not in general followed by a $\sim$ 30-s decay toward a pre-event level, as is usually the case for the VLF signals. Test particle modeling of the whistler-particle interaction supports the idea that the MF signals are affected by ionization extending above the nominal ~85-km reflection height for VLF signals and also are consistent with the observed time delay between the 780-kHz signal perturbation and the whistler-generating lightning stroke. Fast phase advances correlated with the whistlers were regularly observed on a 12.9-kHz Omega signal. The data provide a means of inferring the existence of multiple precipitation regions and offer new evidence that whistlers originating in the northern hemisphere can cause significant precipitation in the southern hemisphere, at least in the vicinity of the South Atlantic magnetic anomaly.

1. INTRODUCTION

Increasing attention is now being devoted to the problem of the pitch angle scattering and resulting precipitation of magnetospheric energetic electrons by coherent waves. Among the phenomena of interest is the "Trimpi" effect, in which the amplitude or phase of a subionospherically propagating VLF signal is perturbed at the time of reception of a magnetospheric whistler. Typical changes on paths 2000–10,000 km in length are ~1–2 dB in amplitude and a few microseconds in phase delay, developing within a time of ~1–2 s and decaying over periods of ~10-100s [*Helliwell et al.*, 1973; *Lohrey and Kaiser*, 1979]. The evidence strongly suggests that these signal perturbations are due to precipitation induced by the correlated whistlers, which scatter particles of sufficient energy to cause an ionization density enhancement below 85 km altitude, the approximate reflection height for VLF waves under nighttime conditions in the earth-ionosphere waveguide [e.g. *Deeks*, 1966]. The process is shown schematically in Figure 1, where the magnetospheric path for a lightning-generated whistler, a subionospheric signal path, and the perturbation caused by whistler-induced precipitation are shown. A test particle model of the gyroresonant whistler-particle interaction in the magnetosphere has been applied to the parameters of an observed case [*Chang and Inan*, 1983]. For a broad range of assumptions about the particle distribution, the results were in accord with both the premise of substantial energy deposition near and below 85 km and the measured time delay between the whistler and the subionospheric signal perturbation.

Recent research based on data from Palmer Station, Antarctica ($L \sim 2.4$) showed that the Trimpi effect can occur well within the plasmasphere, particularly in the aftermath of moderate to severe magnetic disturbances [*Carpenter and LaBelle*, 1982]. These observations have focused attention upon questions such as the spatial distribution of the ionospheric regions perturbed by individual whistlers and the frequency range over which subionospheric signal perturbations can be detected. Frequencies well above VLF are of interest because they probe altitudes above VLF reflection heights and thus may provide information on the vertical profile of the ionization enhancements.

The purpose of this paper is to report the first evi-

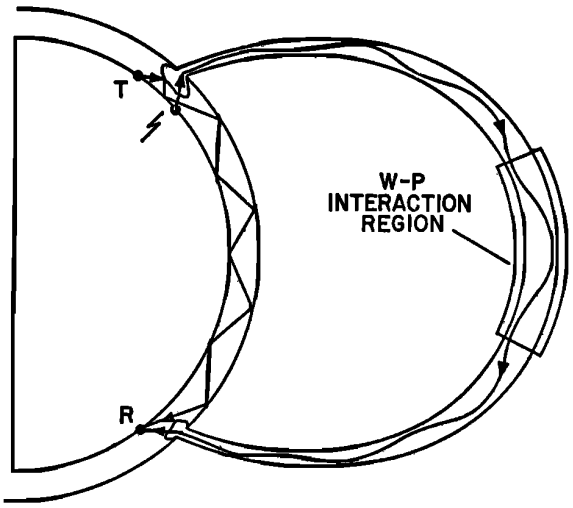

Fig. 1. Sketch depicting the path of propagation of the magnetospheric whistler, a subionospheric propagation path between the source and the receiver, and ionospheric perturbations caused by the whistler-induced particle precipitation.

Paper number 4A0854.
0148-0227/84/004A-0854$02.00

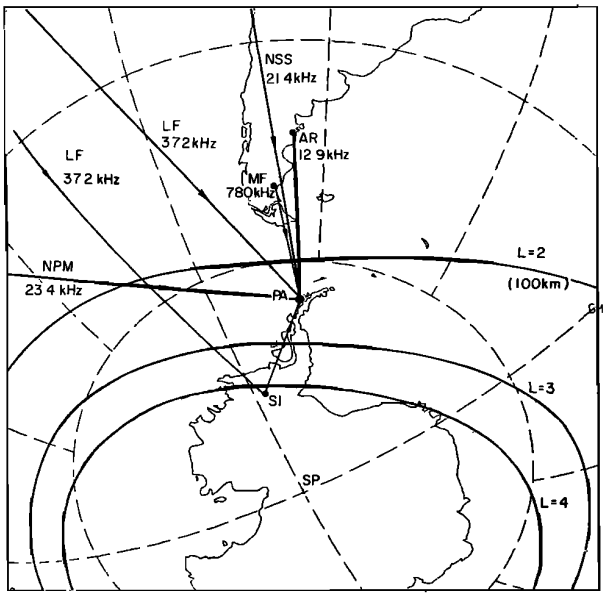

Fig. 2. Map showing examples of great circle paths from various signal sources to Palmer (PA) and Siple (SI) stations, Antarctica.

dence of a correlation between whistlers and amplitude perturbations on low-frequency (LF) signals at 37.2 kHz and medium-frequency (MF) signals at 780 kHz. Differences in the decay of the MF and VLF perturbations suggest that the MF signals are affected by ionization enhancements extending above the nominal 85-km reflection height for VLF. We also report initial observations of phase perturbations on 12.9-kHz Omega navigation signals. The locations of the observing stations Siple and Palmer, Antarctica, as well as great circle paths from several signal sources of interest, are indicated on the map of Figure 2. The locations of all the signal sources of interest are shown in Table 1.

2. Experimental Results

Observations at LF and MF Frequencies

Figure 3, upper trace, shows a 10-min period of negative amplitude perturbations on 37.2 kHz observed at Siple Station. Much of the fine structure is due to multiple whistler events of varying amplitude; for example, the two-stage decreases at ~0824 and 0828 UT (arrows) are a result of corresponding spacing in the associated whistlers. Below is an NSS record showing small positive changes at times that are not in general coincident with the changes on 37.2 kHz.

Figure 4 shows 37.2-kHz signal perturbations observed at Palmer Station on March 30, 1983. In this case there were simultaneous changes on NSS (second panel) as well as small negative perturbations on NPM at 23.4 kHz (third panel).

At Palmer, amplitude changes on 37.2 kHz have been found to occur as frequently as do perturbations on NSS at 21.4 kHz. NSS was previously found to show the largest and most frequent Trimpi effects among the several signals near 20 kHz that were monitored [*Carpenter and LaBelle*, 1982]. In the period March 3 to April 7, 1983, Trimpi events on NSS at 21.4 kHz were detected on the Palmer analog charts on 25 of 36 recording days. Events on 37.2 kHz occurred on 26 of the 36 days.

Trimpi effects on 780-kHz signals originating at Santa Cruz, Argentina (50°S, 69°W), and observed at Palmer on March 30, 1983, are illustrated in the bottom panel of Figure 4. On the other panels, the changes at a given frequency are consistent in sign and show the fast rise (~1–2 s) and slow decay (~30–60 s) that are typical for signals near 15–20 kHz [*Helliwell et al.*, 1973]. In contrast, the 780 kHz record at first shows no clear changes until ~0546 UT. Then alternating negative and positive perturbations occur until ~0600 UT, after which the faster changes are negative. The perturbations at 780 kHz correlated with those on the other records are of order 50% in amplitude and are clearly more rapid than most other variations in the 780-kHz data of comparable magnitude. However, they are not followed immediately by near-exponential decay to an approximately pre-event level, as in the VLF-LF cases shown. Instead there are brief periods of roughly constant amplitude which last ~30 s or longer, followed in this particular case by rising trends.

Figure 5 illustrates the correlation between whistlers and several strong perturbations on a 780-kHz signal recorded at Palmer on March 9, 1983. This case resembled that of Figure 4, in that there were well-defined events on NSS, 37.2 kHz, and Argentina Omega as well as small perturbations on NPM. The top panel in Figure 5 is a voltage-controlled oscillator (VCO) record showing 780-kHz signal amplitude on a linear scale, while the second panel shows the corresponding 0–10 kHz frequency-time spectrum. Arrows above the record show the times of three negative and one positive signal level changes that coincided with strong multicomponent whistlers. Two of these whistler events are shown on expanded records below, where the VCO output for the 780-kHz is also displayed on a compressed amplitude scale. The times of origin of the lightning strokes that generated the whistlers are marked by arrows. The second record contains two whistlers separated in time by ~1 s. The observed delay between the time of origin of the whistler in the first record and the beginning of the perturbation on the 780-kHz signal is ~0.6 s. This is interpreted in the next section in the context of a test particle model of the whistler-induced scattering process.

A notable feature of the MF perturbations is that while

TABLE 1. List of Transmitters

Transmitter	Location	Latitude	Longitude	Frequency
NSS	Maryland	39°N	76°W	21.4 kHz
NPM	Hawaii	21°N	158°W	23.4 kHz
LF (37.2 kHz)	California	35°N	117°W	37.2 kHz
MF (780 kHz)	Argentina	50°S	69°W	780 kHz
Omega	Argentina	43°S	65°W	12.9 kHz

they tended to occur on nights of high activity on the VLF/LF signals, the number of observed events per night was generally less than 10, much smaller than the total of > 50 typically observed on signals such as NSS.

Phase Perturbations on Argentina Omega Signals

Figure 4 (top panel) shows results obtained at Palmer using a phase-tracking receiver to observe the Argentina Omega signal at 12.9 kHz, which has a ~ 40% duty cycle. An integration time constant of ~2.5 s for the phase-tracking receiver has been found sufficient for identification of events. The panel shows a series of phase advances coincident with the perturbations on the amplitude records just below. In this case the advance is ~ 0.7 μs, or ~ 3 electrical degrees over the ~2400 km path (see map of Figure 2). The occurrence rate of phase changes on Argentina Omega at Palmer was found to be comparable to that of the most frequently observed amplitude changes on other sources. During the period in March–April 1983 mentioned above, phase changes were detected on 18 of 35 recording days.

In contrast to the readily detectable phase changes, amplitude perturbations on the Argentina Omega 12.9-kHz signal were only marginally detectable, ranging when observed from ~0.04 db to 0.2 db.

3. DISCUSSION

The phase perturbations on the 12.9-kHz Omega signal and the amplitude perturbations on the 780-kHz path at Palmer provide additional evidence that whistlers originating in the northern hemisphere can cause significant precipitation in the southern hemisphere [*Rosenberg et al.*, 1971; *Helliwell et al.*, 1980; *Carpenter and LaBelle*, 1982], a process that is probably aided by the north-south mirror height asymmetry at the Palmer-Siple longitudes. Because of this asymmetry [*Barish and Wiley*, 1970], particles mirroring in the region conjugate to Palmer at 450 km altitude can reach 100 km over Palmer.

The results shown in Figure 4 clearly indicate that several paths representing a ~ 90° range of arrival bearings are

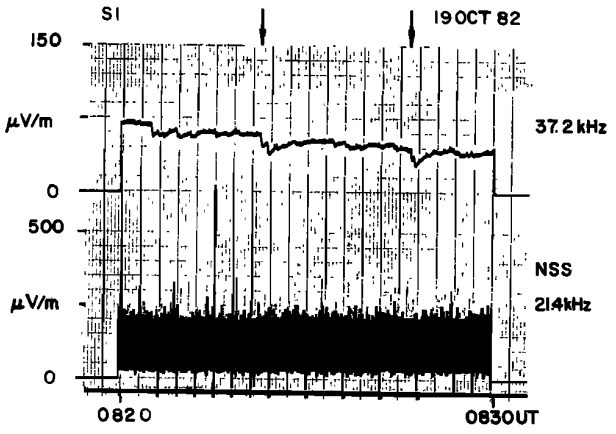

Fig. 3. Amplitude records from Siple, Antarctica, showing negative amplitude perturbations on 37.2 kHz (upper trace) and positive changes on NSS at 21.4 kHz.

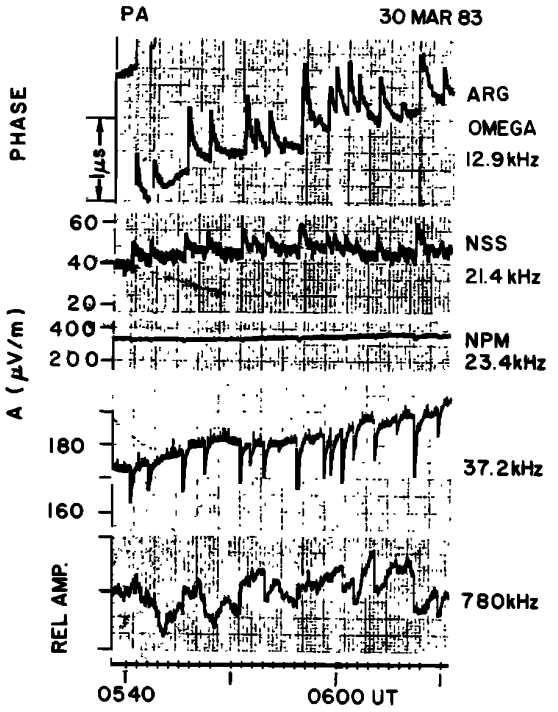

Fig. 4. Chart record from Palmer, Antarctica, showing simultaneous perturbations on a wide range of frequencies, from 12.9 kHz to 780 kHz. The top record displays the phase of the Omega Argentina signal at 12.9 kHz, while the others show amplitude.

simultaneously perturbed. The spatial distribution of precipitation regions in the ionosphere corresponding to events such as those of Figure 4 is not known. An outstanding question is the extent to which each major component in an individual whistler produces a separately identifiable precipitation region. In an earlier study of Palmer data on NSS and NLK (arrival bearing 319°), *Carpenter and LaBelle* [1982] inferred that the precipitation regions affecting individual signals were ~100 km in east-west extent. The regions were estimated to be located up to ~400 km equatorward of the station and within ~200 km of the affected great circle paths, but did not in general overlap the paths. On this basis, the observation at Palmer of perturbations on a pair of signals such as 37.2 kHz and NSS might be attributed to a single precipitation region located several hundred kilometers from the station and in a direction between the affected great circle paths. However, the occurrence of simultaneous perturbations on NPM, 37.2 kHz, and NSS (see map of Figure 2) suggests that in such cases, multiple precipitation regions may be involved, distributed both in latitude and longitude over distances of the order of 500 km (for reference, the Siple to Palmer distance is ~1400 km).

The lack of simultaneity of the 37.2-kHz and NSS perturbations at Siple in Figure 3 may be attributed to longitudinally spaced ionospheric regions excited by independent (and hence uncorrelated) lightning sources. Preliminary calculations suggest that these regions are preferentially located at $L < 3.5$. A detailed study of the Siple data is now in progress and will be reported later.

The lack of a ~30–60 s recovery to pre-event levels fol-

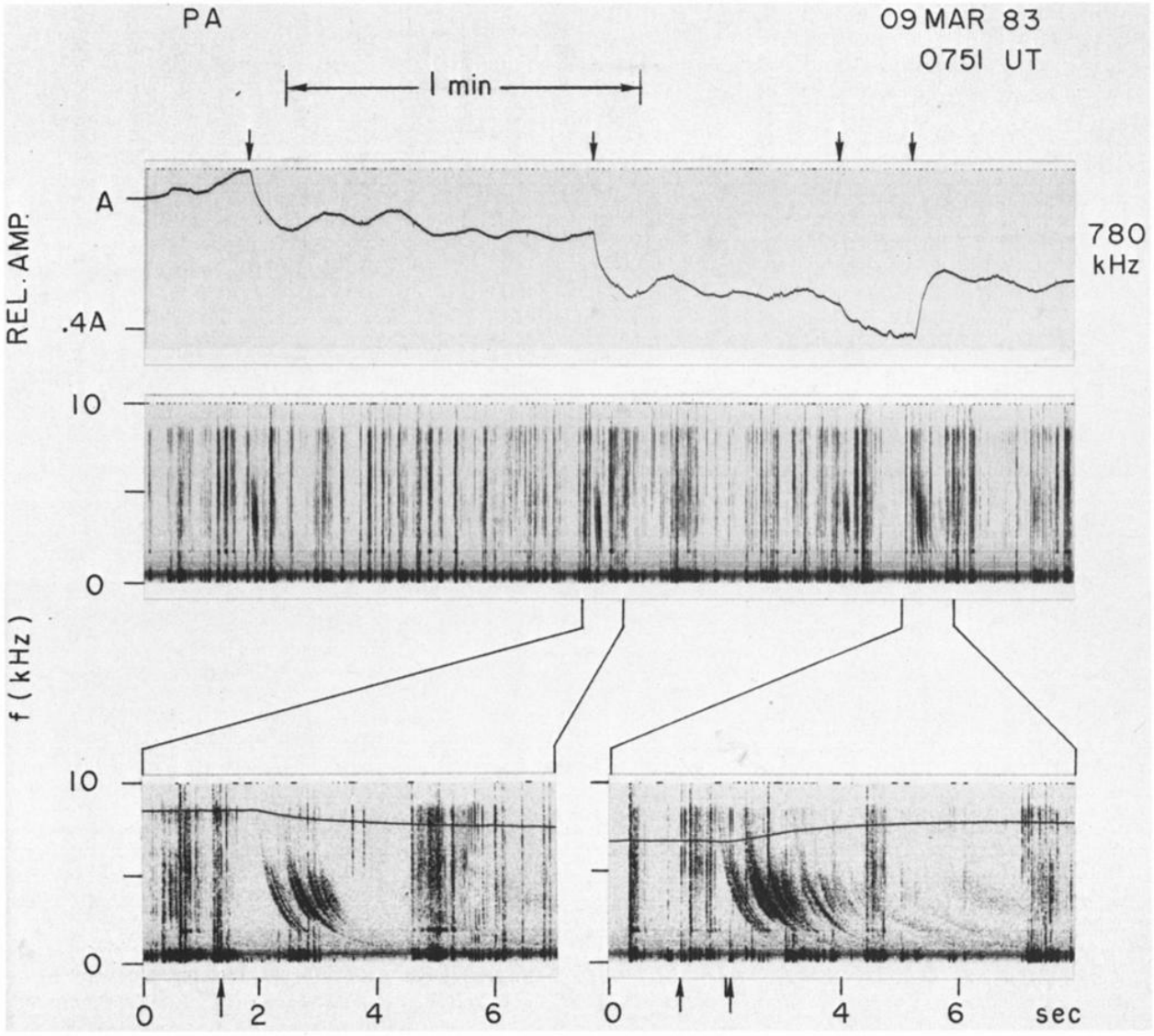

Fig. 5. Example of a correlation between whistlers and several 20–40 % perturbations on a 780-kHz signal recorded at Palmer, Antarctica. The upper two panels compare the 780-kHz signal amplitude with the 0 - 10 - kHz frequency-time spectrum showing whistlers during a 2.5-min period. Arrows above the record show the times of signal level changes that coincided with strong multicomponent whistlers. Two of these whistler events are shown on an expanded record below. The times of origin of the lightning strokes that generated the whistlers are marked by arrows.

lowing the 780-kHz perturbations at Palmer in Figures 4 and 5 is tentatively attributed to the penetration of the signals to altitudes above the ~85 km reflection level of the VLF and 37.2-kHz signals. On the Santa Cruz to Palmer path, reflection for one-hop ionospheric propagation at 780 kHz is estimated to occur at ~90 km for nighttime conditions. Near 90 km, the recovery time for excess ionization is expected to be of the order of minutes [*Cladis et al.*, 1973; *Smith et al.*, 1974], as opposed to the ~30–60 s recovery inferred to occur near 85 km from the VLF events. (The difference is believed to be associated with a change with altitude in the type of process governing decay of excess electrons [*Dingle*, 1977]. Above 80–85 km the decay is governed by an effective recombination coefficient which depends upon the rates at which both electrons and negative ions combine with positive ions, while below 80–85 km it is dominated by the attachment rate of electrons to neutral molecules.) Thus it appears that in the cases shown in this paper, significant enhancements of the ambient nighttime ionization profile may have occurred up to at least ~90 km altitude.

The occasional alternations in sign of the perturbations seen at 780 kHz (Figures 4 and 5) might be explained as follows. The 780-kHz path is ~ 1800 km long, too long for significant ground wave strength, but favorable for one- and two-hop sky wave rays. (The presence of two waves of comparable amplitude is suggested by relatively deep fading of the signal on a time scale of 10–20 min.) If the region of precipitation includes only one reflection point, a phase shift between the one-hop and two-hop rays would occur, causing fading. Since the recovery time appears to exceed the time

between events, successive phase shifts would tend to be cumulative. If the total change in phase path per event approaches $\sim \lambda/2$, then each successive event would tend to reverse the phase of the affected ray, causing alternating increases or decreases in total received field intensity.

Support for this hypothesis is found in the $\sim 0.7 - \mu$s phase changes on Omega Argentina at 12.9 kHz, shown in Figure 4. At this wavelength ($\sim$ 23 km) the corresponding phase shift is only $\sim 3°$. However, at 780 kHz a comparable phase path change (0.7μs, or 0.21 km) produces a phase change of 200°. quite close to the required one-half wavelength. Modeling studies of the MF behavior, as well as additional experimental data, are clearly required.

In order to determine the energy range of the electrons precipitated by the whistlers of Figure 5 and to interpret the observed $\sim$0.6 s delay between the time of origin of the whistler and the beginning of the perturbation on the 780-kHz signal, a test-particle model of the whistler-particle interaction [*Inan et al.*, 1982; *Chang and Inan*, 1983] was applied to the parameters of this case. The relevant path parameters $L = 2.1 \pm 0.1$ and $N_{eq} = 3200 \pm 300$ cm^{-3} were obtained from analysis of the initial component of several whistlers correlated with 780-kHz perturbations. The later-arriving whistler components propagated at L values equal to or larger than that of Palmer and thus should not have affected the 780-kHz signal. A whistler frequency range of 1.5–8 kHz was assumed, based on the range of component definition on spectrograms.

The results of using the test particle model of the whistler-particle interaction for these data are shown in Figure 6. The top panel shows the normalized energy flux as a function of time as observed in the southern hemisphere, where $t = 0$ is the time of origin of the lightning stroke that generated the whistler. The whistler is assumed to originate in the northern hemisphere and interacts with the electrons as it travels southward. The particles that are pitch angle scattered as a result of this interaction first travel to the northern hemisphere, where they mirror back due to the relatively high local mirror altitudes (at longitudes near the South Atlantic magnetic anomaly). They then precipitate into the ionosphere in the southern hemisphere, where they first arrive $\sim$ 0.58 s after the lightning stroke. This result is in good agreement with the time to onset of the 780-kHz perturbation shown in Figure 5 and provides additional evidence of the causative role of whistlers in the 780-kHz perturbations (in Figure 5, the rise time of the perturbations is distorted by the effects of filtering used in obtaining the VCO display).

The energy range of the computed flux as shown in the lower panel of Figure 5 is also supportive of the inferences drawn from the data. To a first approximation the precipitation energy flux is uniformally distributed over the 70 190 keV range. A large fraction of the particles in the energy range 70-100 kev would be deposited at 90 km altitude [*Banks et al.*, 1974], and could therefore have produced the density enhancements inferred to be generated at these altitudes. It should be noted that while the magnitude and energy spectra of the computed fluxes are dependent in part on the model parameters listed in the caption for Figure 6, the timing relationships are not sensitive to the assumed values of those parameters. Among the parameters, the trapped energetic particle distribution, which for the present case

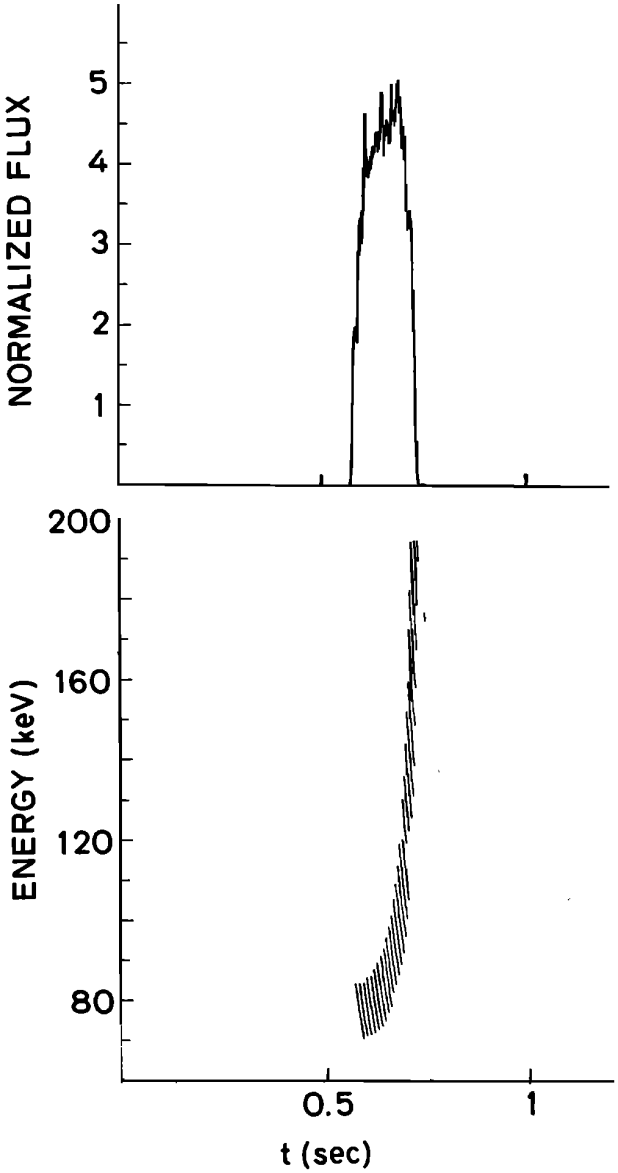

Fig. 6. Computed precipitation flux induced by a whistler propagating at $L = 2.1$ and for an equatorial cold plasma density of 3200 el/cc. The upper panel shows normalized flux as a function of time, whereas the lower panel gives the energy of the particles that constitute the flux [*Inan et al.*, 1982]. The whistler is assumed to cover a frequency range of 1.5–8 kHz and to have entered the medium at 1000 km altitude at $t = 0$ (the time of the lightning stroke). The input signal is assumed to have a constant power spectral density over the range 1.5–8 kHz, so that the equatorial wave intensities corresponding to lower frequencies are smaller due to higher dispersion. The total energy of the wave packet is taken to be equivalent to that of a monochromatic pulse of duration 0.1 s and equatorial wave intensity of 5 pT. The energetic particle distribution was assumed to be proportional to E^{-3}, where E is the particle energy. For further details of the model calculations the reader is referred to *Chang and Inan* [1983].

was assumed to be proportional to E^{-3}. determines the relative amounts of flux at various particle energies. However. in the absence of information on absolute flux levels. this dependence does not influence our present findings.

4. SUMMARY

1. Whistler-correlated amplitude perturbations were observed on 37.2-kHz LF paths from the northern hemisphere to Palmer ($L \sim 2.4$) and Siple ($L \sim 4.3$), Antarctica. The occurrence rates were comparable to those observed on VLF sources at ~20 kHz. Examples were seen on 70% of the nights during a 36-day period in March–April 1983.

2. Whistler-correlated amplitude perturbations were observed on a 780-kHz MF signal propagating on a ~ 1800 km path from South America to Palmer. Events tended to occur on nights of high activity on VLF signals, but the number of observed events on such nights was generally less than 10, much smaller than the total of >50 typically observed on signals such as NSS at 21.4 kHz.

3. The observed MF perturbations were of order 50% in amplitude and developed much more quickly than other changes of comparable magnitude on the signal. The MF perturbations were not in general followed by a ~30-s decay toward a pre-event level, as is usually the case at the VLF frequencies. This is interpreted as evidence that the MF signals are affected by ionization enhancements extending above the nominal 85-km ionospheric reflection height for VLF signals. Model calculations support this picture, and also provide a consistent interpretation of the observed time delay between the subionospheric signal perturbation and the whistler-generating lightning stroke.

4. Fast phase advances correlated with whistlers were regularly observed on the Omega Argentina 12.9-kHz signal propagating to Palmer on a ~ 2400-km path. The occurrence rate was comparable to that of the more frequent amplitude changes on other VLF sources. Amplitude perturbations on the Omega Argentina signal were only marginally detectable.

5. Simultaneous perturbations on signal paths with arrival bearings ranging over ~90° at Palmer suggest that multiple precipitation regions exist, distributed both in latitude and longitude over distances of order 500 km.

6. Perturbations on the ~ 2000 km southern hemisphere 12.9-kHz and 780-kHz paths from Argentina to Palmer provide additional evidence that whistlers originating in the northern hemisphere can cause significant precipitation in the southern hemisphere. This effect is believed to be enhanced by the presence of the South Atlantic magnetic anomaly. In order to assess the effect of the conjugate mirror height asymmetry in determining the occurrence rate, amplitude, and frequency range of the Trimpi effect, comparative studies should be made in regions away from the anomaly.

Acknowledgments. We thank our colleagues at STAR laboratory for their support and H. C. Chang for his help in connection with the result given in Figure 6. We also thank M. Dermedziew and T. Wolf for their work at Siple Station and J. Yarbrough and P. Pecen for assistance in data analysis and display. The typescript was prepared by G. Walker, N. Leger, and B. Fortnam. This work was supported by the Division of Polar Programs of the National Science Foundation under grants DPP-82-17820 and DPP-80-22282 and by the National Aeronautics and Space Administration under grant NGL-05-020-008.

The editor thanks Bruce Edgar and another referee for their assistance in evaluating this paper.

REFERENCES

Banks, P. M., C. R. Chappell, and A. F. Nagy, A new model for the interaction of auroral electrons with the atmosphere: spectral degradation, backscatter, optical emission, and ionization, *J. Geophys. Res., 79*, 1459, 1974.

Barish, F. D., and R. E. Wiley, World contours of conjugate mirror locations, *J. Geophys. Res., 75*, 6342, 1970.

Carpenter, D. L., and J. W. LaBelle, A study of whistlers correlated with bursts of electron precipitation near $L = 2$, *J. Geophys. Res., 87*, 4427, 1982.

Chang, H. C., and U. S. Inan, Quasi-relativistic electron precipitation due to interactions with coherent VLF waves in the magnetosphere, *J. Geophys. Res., 88*, 318, 1983.

Cladis, J. B., G. T. Davidson, W. E. Francis, L. L. Newkirk, and M. Walt, Ionospheric disturbances affecting radio-wave propagation, *Final Rep. DNA 3103F*, Lockheed Palo Alto Res. Lab., Palo Alto, Calif., 1973.

Deeks, D. G., *D*-region electron distributions in middle latitudes from the reflection of long radio waves, *Proc. R. Soc., London, Ser. A, 291*, 413, 1966.

Dingle, B., Burst precipitation of energetic electrons from the magnetosphere, Ph.D. thesis, Stanford Univ., Stanford, Calif., 1977.

Helliwell, R. A., J. P. Katsufrakis, and M. L. Trimpi, Whistler-induced amplitude perturbation in VLF propagation, *J. Geophys. Res., 78*, 4679, 1973.

Helliwell, R. A., S. B. Mende, J. H. Doolittle, W. C. Armstrong, and D. L. Carpenter, Correlations between λ4278 optical emissions and VLF wave events observed at $L \sim 4$ in the Antarctic, *J. Geophys. Res., 85*, 3376, 1980.

Inan, U. S., T. F. Bell, and H. C. Chang, Particle precipitation induced by short duration VLF waves in the magnetosphere, *J. Geophys. Res., 87*, 6243, 1982.

Lohrey, B., and A. B. Kaiser, Whistler-induced anomalies in VLF propagation, *J. Geophys. Res., 84*, 5121, 1979.

Rosenberg, T. J., R. A. Helliwell, and J. P. Katsufrakis, Electron precipitation associated with discrete VLF emissions, *J. Geophys. Res., 76*, 8445, 1971.

Smith, L. G., M. A. Geller, H. D. Voss, Energetic electrons in the mid-latitude nighttime *E* region, *J. Atmos. Terr. Phys., 36*, 1601, 1974.

D. L. Carpenter, U. S. Inan, M. L. Trimpi, R. A. Helliwell, and J. P. Katsufrakis, Space, Telecommunications, and Radioscience Laboratory, Stanford University, Stanford, CA 94305.

(Received March 28, 1984;
revised June 6, 1984;
accepted June 11, 1984.)